Sahel Rainfall variability and response to Greenhouse Warming

Reindert Haarsma, Frank Selten, Nanne Weber, Michael Kliphuis

Royal Netherlands Meteorological Institute,

P.O. Box 201, 3730 AE De

Bilt, The Netherlands

e-mail: haarsma@knmi.nl

Abstract

The NCEP/NCAR re-analyses as well as ensemble integrations with an atmospheric GCM indicate that interannual variations in Sahel rainfall are related to variations in the mean sea level pressure (MSLP) over the Sahara. In turn the MSLP variations are related to the global distribution of surface air temperature (SAT). An increase in SAT over the Sahara, relative to the surrounding oceans, decreases the MSLP over the Sahara, thereby increasing the Sahel rainfall. We hypothesize that through this mechanism greenhouse warming will cause an increase in Sahel rainfall, because the warming is expected to be more prominent over the summer continents than over the oceans. This has been confirmed using an ensemble of 62 coupled model runs forced with a business as usual scenario. The ensemble mean increase in Sahel rainfall between 1980 and 2080 is about 1-2 mm day^{-1} (25-50%) during July-September, thereby strongly reducing the probability of prolonged droughts.

Introduction

The Sahel region is a semi-arid region which has experienced large decadal fluctuations in rainfall including prolonged periods of drought. Two contrasting hypotheses concerning the cause of these droughts have been put forward: variations in sea surface temperatures (SSTs) (Folland et al. 1986, Rowell et al. 1995, Ward 1998, Janicot et al. 2001) and the effect of human activity on the surface vegetation (Xue and Shukla 1993, Clark et al. 2001). Especially the latter has been mentioned as a primary cause for the drought during the 70-90s. However, recent modelling studies provided strong evidence that SST fluctuations primarily caused this drought period. The observed decadal fluctuations during the last 50 years in Sahel rainfall are reproduced in simulations with atmospheric GCMs forced by observed SSTs (Giannini et al. 2003, Rowell 1996, Bader and Latif 2003). Land-surface feedbacks mainly seem to amplify the SST-induced changes (Taylor et al. 2002, Zeng et al. 1999).

Although the link between SSTs and decadal Sahel rainfall fluctuations is rather well established and plausible mechanisms have been put forward in numerous studies, there still remain significant questions about how the global SST distribution affects the atmospheric circulation and subsequently the Sahel rainfall. This will be the focus of the first part of this article. In the second part we will show that a similar mechanism leads to an increase in Sahel rainfall in response to anthropogenic warming.

Historical Sahel rainfall variability

To investigate the historical Sahel rainfall variability we used the NCAR atmospheric GCM CCM3 in T31L18 resolution (Kiehl et al. 1998). Using observed SSTs from 1945 onwards (Reynolds and Smith 1994) in an ensemble of 10 members we were able to simulate the historical decadal variations in the Sahel including the drought during the 70-90s, although the modeled decline in rainfall is less than observed (Fig.1). The correlation of the area mean rainfall at 10^{o}N-20^{o}N, 10^{o}W-30^{o}E during July-August-September (JAS) between the ensemble mean and the CRU TS 2.1 data set (Mitchell and Jones 2005) is 0.48 for annual data and 0.89 after applying a 10-yr running mean. Similar results were first obtained by Rowell et al. (1996) and later by Giannini et al. (2003).

For these SST-forced experiments an analysis of the covariability of rainfall and mean sea level pressure (MSLP) over northern Africa during JAS, by means of a singular value decomposition (SVD) analysis, reveals that anomalous large Sahel rainfall is related to an anomalous low centered over the northeast Sahara (Fig. 2a). The rainfall as well as the MSLP pattern (referred to as the Sahara Low) of the SVD analysis are very similar to the dominant empirical orthogonal functions (EOF) of rainfall and MSLP over this region (not shown), which explain respectively 18% and 47% of the interannual variations. The southern meridional pressure gradient of the Sahara Low induces, in case of a negative phase, enhanced moisture advection from the southwest thereby increasing the Sahel rainfall (Fig. 2a).

We checked these results for the NCEP/NCAR reanalysis (Kalnay et al. 1996) and the CMAP rainfall data (Xie and Arkin 1996). We note here that Janicot et al. (2001) and Rowell (2003) discuss the problems of the NCEP/NCAR reanalysis over this region and advise not to use it before 1968. A similar SVD analysis (Fig. 2b) confirms the relation between the MSLP distribution over the northeastern part of the Sahara and the Sahel rainfall. Both the interannual fluctuations as well as the decreasing trend in Sahel rainfall during the 70-90s are well correlated with changes in the amplitude of the Sahara Low.

We next turn to the question what determines the variability of the Sahara Low. A regression analysis of the amplitude of the Sahara Low with global surface air temperatures (SAT) (Fig. 3ac) reveals similar patterns for the SST-forced runs and the NCEP/NCAR reanalysis. These patterns indicate that on interannual time scales a deeper Sahara Low is related to warmer temperatures over the Sahara and the Eurasian continent. The SAT over the Sahara shows a strong gradient at the border with the Sahel zone, where increased rainfall, cloudiness and bottom moisture result in a decrease in SAT. The southern gradient in MSLP of the Sahara Low, which determines the anomalous moisture flux, is associated with this large gradient in SAT. Over the equatorial Pacific a strong ENSO signal is visible. The importance of ENSO for Sahel rainfall has been documented in several studies (Rowell et al. 1995, Janicot et al. 2001).

On decadal time scales the regression analysis for the runs with prescribed SSTs shown in Fig. 3b reveals a much weaker ENSO signal, but in addition shows a significant contribution from the Indian and South Atlantic ocean SSTs as was also observed by e.g.

Folland et al. (1986), Rowell et al. (1995) and Giannini et al. (2003). The Northern Hemisphere continental heating still remains significantly correlated with the Sahara Low.

The effect of SSTs on Sahel rainfall has been explored extensively in previous studies, whereas up to now the role of continental surface temperatures has not yet been considered. Viewed from the perspective of forecasting the Sahel rainfall this is logical, because due to the large heat capacity of water there is a much larger potential predictability for SSTs than for land surface temperatures. However Fig. 3 suggests that the MSLP distribution over the Sahara, and therefore the Sahel rainfall, depends on the temperature difference between the continents and the oceans: enhanced Sahel rainfall on decadal time scales is related to warm Northern Hemisphere continents and cool Southern Hemisphere oceans (Fig. 3b).

These results suggest that the anthropogenic changes in Sahel rainfall will depend on the spatial structure of the anthropogenic warming, which will be explored below.

Anthropogenic changes

For studying the anthropogenic changes we used the NCAR CSM 1.4 model, where CCM3 is coupled to an ocean model, which has 25 vertical levels and 3.6^{o} longitudinal resolution. The latitudinal resolution ranges from 0.9^{o} in the tropics to 1.8^{o} at higher

latitudes. No artificial corrections in the heat exchange between atmosphere and ocean are applied.

The simulation period is 1940-2080. Until 2000 the forcing includes temporally evolving estimates of solar radiation, volcanic aerosols and major greenhouse gases (GHGs). From 2000 onwards all these forcings are kept constant, except for the GHGs, which increase according to a "business-as-usual" (BAU) scenario (Dai et al. 2001), similar to the SRES-A1 scenario. An ensemble of 62 simulations was produced, each differing in a small random perturbation to the initial atmospheric temperature field (Selten et al. 2004).

The SVD analysis of Sahel rainfall and MSLP of the coupled integrations for the control period from 1940-2000 yielded very similar patterns as obtained in the SST forced runs (not shown). Also the regression of the Sahara Low with SAT reveals similar patterns although the signal over the oceans is reduced due to an underestimation of SST variability in the coupled model especially on decadal time scales. The main difference is the absence of the ENSO signal, which is probably due to the different characteristics of the ENSO simulated by the model (Zelle et al. personal communication).

Over the tropics and subtropics the ensemble mean anthropogenic warming at the end of the integration period (Fig. 4a) is less over the oceans compared to the continents. This is mainly due to the reduction in net surface solar radiation, which is larger over the oceans (4 Wm^{-2}) than over the continents (2.5 Wm^{-2}). This reduction is related to an increase of low-level clouds, which is about 4 % over the oceans. Over the continents the increase is

much less. Over Australia there is enhanced heating due to drying-out of the bottom. For the Sahara this mechanism does not play a role, because, with a latent heat flux of about 1 Wm^{-2}**,** it is already almost completely dry at the beginning of the integration period. The contribution of the thermal inertia to the reduced warming of the oceans appears to be small: during the period of linearly increasing GHG forcing the SAT difference between the oceans and the continents increases linearly without leveling-off. This is to be expected for the limited heat content of the mixed layer in the tropics and subtropics. We cannot rule out the possibility of a slow surface ocean response due to changes in the deep ocean because of the shortness of the integrations. However, Meehl et al. (Personal communication) show for the CCSM3 climate model a similar difference in warming between the oceans and the continents, that does not reduce if the model is integrated for another 100 years after stabilization of the GHG emissions.

Neelin et al. (2003) propose the "upped-ante" mechanism. In case of greenhouse warming the atmosphere will be able to contain more moisture. While in regions of deep convection the moisture supply will always be sufficient, regions at the margins of convection may not be able to meet the "upped-ante', due to an atmospheric circulation that advects dry air from non-convective regions into such margins. Analysis of the moisture budget reveals that indeed at the northern boundary of the Sahel rainfall zone the drying caused by $\hat{\mathbf{v}}.\nabla\hat{q}$ counteracts the moistening due to the monsoon effect $\mathbf{v'}.\nabla\hat{q}$ caused by the deeper Sahara Low, both terms being of the same order of magnitude. Without the "upped-ante" mechanism, the Sahel rainfall zone would have shifted even further northward. The air that is advected from the non-convective region into the

margins is also hot, which causes the enhanced warming just north of the Sahel rainfall zone (Fig.4a).

Due to the heating over the Sahara we expect a decrease in MSLP over the Sahara and a subsequent increase in Sahel rainfall, similar as for the historical Sahel rainfall variations. Figs. 4ab show that indeed there is a decrease in MSLP of about 0.5 hPa over the Sahara and an increase in the order of 1-2 mm day^{-1} (25-50%) in Sahel rainfall during JAS. The pattern of anthropogenic change in Sahel rainfall is very similar to the dominant pattern of interannual Sahel rainfall variability. The decrease in rainfall south of the Sahel caused by anthropogenic warming is also observed in the dominant pattern of rainfall variability for the coupled runs. This is not seen in the SST-forced runs (Fig. 2a), possibly due to the different rainfall climatology.

To test the hypothesis that an enhanced heating of the Sahara deepens the Sahara Low, thereby increasing the Sahel rainfall due to the increased moisture transport into the Sahel region, we performed an additional experiment. We compared a 30-year control integration of the atmospheric model with prescribed SSTs computed from the coupled integration for the period 1960-1960, with a similar integration in which we applied an enhanced heating of 4 Wm^{-2} over the Sahara. This heating is stronger than the anomalous land-sea contrast of about 1.5 Wm^{-2} at the end of the integration period in order to obtain a clear result from this sensitivity experiment. Due to this heating the temperature over the Sahara increases about $1^{o}C$ and Fig.4c shows that for JAS this indeed causes an

anomalous low over the Sahara and an anomalous rainfall pattern that is very similar to the anthropogenic pattern in the coupled model (Fig. 4b). The amplitude of the anomalous rainfall pattern in this experiment is about a factor of 2 stronger than the anthropogenic increase in the coupled integration, which is in agreement with the stronger increase in SAT over the Sahara and the resulting deeper Sahara Low.

Fig. 4a reveals that not only the Sahara, but the whole Eurasian continent has warmed. To verify if the Eurasian warming affects the Sahel rainfall we did a similar experiment as described above, but now for the Eurasian continent. For a heating of 10 Wm^{-2} extending from Europe to 90^{o}E, between 30^{o}N and 55^{o}N the temperature increase is about 1^{o}C However, no significant change in MSLP over the Sahara and Sahel rainfall was observed. From this we conclude that the Eurasian heating does not play a significant role for the Sahel rainfall.

The probability of dry years strongly diminishes during the end of the integration period as shown in Fig. 5a. The probability of a year with less than 3.5 mm day^{-1} of rain during JAS reduces from about 15% to 3%. Due to natural variability individual ensemble members show prolonged wet and dry spells. Notwithstanding these fluctuations Fig. 5b reveals a very large probability that the 30-year averaged Sahel rainfall is larger during 2050-2080 than during 1950-1980.

Discussion

Both NCEP/NCAR re-analysis and model simulations suggest that historic Sahel rainfall variability is related to SAT over the Sahara. The question why the Sahara was anomously cool during the drought of the 70-80s lies outside the scope of this study and is subject of ongoing research. We speculate that this caused by a combination of external forcing like solar radiation, aerosols and GHG, cooling the Sahara, together with the internal dynamics of the oceans resulting in warm oceans.

Our coupled GHG simulations suggest that Sahel rainfall increases by 1-2 mm day^{-1} (25-50%) during JAS at the end of this century, caused by an enhanced heating of the Sahara compared to the nearby oceans. Comparable processes have been simulated for past periods of enhanced summer warming (e.g. Tuenter et al., 2003). Climate models seem to underestimate the magnitude of monsoon changes considerably compared to reconstructions based on paleo data (Joussaume et al., 1999), which may be due to the absence of vegetation, soil and lake feedbacks. Therefore, we consider our results of anthropogenic increase in Sahel rainfall as a lower bound for the BAU scenario.

As discussed in the introduction land cover does affect Sahel rainfall, although a quantitative estimate of its influence is still under debate. Whether or not future anthropogenic changes in land use will counteract the simulated increase in Sahel rainfall is an open question.

The difference in heating over the continents and oceans is in this model related to changes in cloud cover. The reliability of these cloud cover changes is difficult to assess. However, the enhanced continental heating appears to be a rather common result among different climate models.

Acknowledgments

M. Kliphuis was funded by CKO., computer resources by NCF and NWO.

References

Bader, J. and M. Latif, The impact of decadal-scale Indian Ocean sea surface temperature anomalies on Sahelian rainfall and the North Atlantic Oscillation. Geophys. Res. Lett., 30, doi: 10.1029/2003GL018426, 2003.

Clark, D.B., Y.K. Xue, R.J. Harding, and. P.J. Valdes, Modeling the impact of land surface degradation on the climate of tropical North Africa. J. Clim., 14, 1809-1822, 2001.

Dai, A., T.M.L. Wigley, B.A. Boville, J.T. Kiehl, and L.E. Buja, Climates of the twentieth abd twenty-first centuries simulated by the NCAR Climate System Model. J. Clim., 14, 485-519, 2001.

Folland, C.K., T.N. Palmer and D.E Parker, Sahel rainfall and worldwide sea temperatures. Nature, 320, 602-607, 1986.

Giannini, A., R. Saravanan and P. Chang, Oceanic forcing of Sahel rainfall on inter-annual to inter-decadal time scales. Science, 302, 1027-1030, 2003.

Janicot, S., S. Trzaska and I. Poccard, Summer SAHEL-ENSO teleconnection and decadal time scale SST variations. Clim. Dyn., 18, 303-320, 2001.

Joussaume, S., and 33 co-authors, Monsoon changes for 6000 years ago: results of 18 simulations from PMIP. Geophys. Res. Letters, 26, 859-862, 1999.

Kalnay, E. et al., The NCEP/NCAR reanalysis 40-year project. Bull. Amer. Meteor. Soc., 77, 437-471, 1996.

Kiehl,J.T., J.J. Hack, G.B. Bonan, B.A. Boville, D.L. Williamson and P.J. Rasch, The National Center for Atmospheric Research Community Climate Model: CCM3. J. Clim., 11, 1131-1149, 1998.

Mitchell, T.D. and P.D. Jones, An improved method of constructing a database of monthly climate observations and associated high-resolution grids. Int. J. Clim., 25, DOI:10.1002/joc.1181, 693-712, 2005.

Neelin, J.D., C. Chou and H. Su, Tropical drought regions in global warming and ENSO teleconnections. Geophys. Res. Lett. 30, 2275, doi:10.1029/2003GL018625, 2003.

Reynolds, R.W., and T.M. Smith, Improved global sea surface temperature analysis using optimal interpolation. J. Clim., 7, 929-948, 1994.

Rowell, D.P., C.K. Folland, K. Maskell and M.N. Ward, Variability of summer rainfall over tropical north Africa (1906-92): Observations and modelling. Q. J. R. Meteorol. Soc., 121,669-674, 1995.

Rowell, D.P., C.K. Folland, K. Maskell and M.N. Ward, Further analysis of simulated interdecadal and interannual variability of summer rainfall over tropical north Africa – Reply. Q. J. R. Meteorol. Soc., 122, 1007-1013, 1996.

Rowell, D.P., The impact of Mediterranean SSTs on the Sahelian rainfall season. J. Clim., 16, 849-862, 2003.

Selten, F.M., G.W. Branstator, H.A. Dijkstra and M. Kliphuis, Tropical origins for recent and future Northern Hemisphere climate change. Geophys. Res. Lett. 31, L21205, doi:10.1029/2004GL020739, 2004.

Taylor, C.M., E.F. Lambin, N. Stephenne, R.J. Harding and R.L.H. Essery, The influence of land use change on climate in the Sahel. J. Clim., 15, 3615-3629, 2002.

Tuenter, E., S.L. Weber, F.J. Hilgen and L.J. Lourens, The response of the African summer monsoon to remote and local forcing due to precession and obliquity. Global and Planetary Change, 36, 219-235, 2002.

Ward, M.N, Diagnosis and short-lead time prediction of summer rainfall in tropical North Africa at interannual and multidecadal timescales. J. Clim.,11, 3167-3191, 1998.

Xie, P and Arkin, P.A., Analyses of global monthly precipitation using gauge observations, satellite estimates, and numerical nodel predictions. J. Climate, 9, 840-858, 1996.

Xue, Y. and J. Shukla, The influence of land surface properties on Sahel climate. Part I: desertification. J. Clim., 6, 2232-2244, 1993

Zeng, N., J.D. Neelin, K.-M. Lau and C.J. Tucker, Enhancement of interdecadal climate variability in the Sahel by vegetation interaction. Science, 286, 1537-1540, 1999.

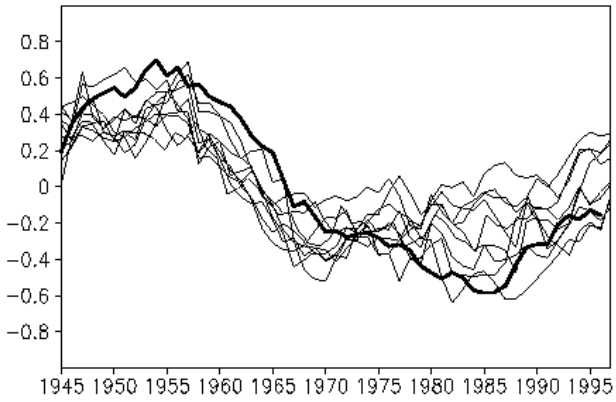

Figure 1. Anomalous rainfall [mm day^{-1}] during JAS for the Sahel region 10^{o}N-20^{o}N, 10^{o}W-30^{o}E. Thin lines: Individual model runs. Thick line: Observations. A 10-yr running mean is applied.

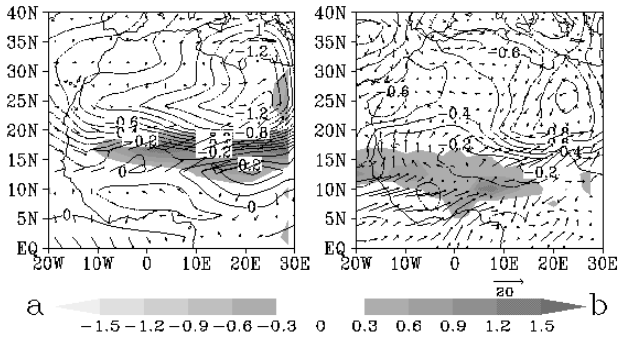

Figure 2. **a**) First SVD mode of anomalous MSLP [hPa] (contours) and rainfall [mm day^{-1}] (shaded) for the 10 ensemble integrations with prescribed observed SST from 1940- 2002. The patterns are normalized to one standard deviation of the PCs. The arrows are the regression of the moisture flux at 925 hPa [(kg.m) $(kg.s)^{-1}$] onto the normalized PC of the MSLP pattern. **b**) As **a** but now for the NCEP/NCAR reanalysis and CMAP data for 1979-2004. The explained total squared covariance in **a** and **b** are respectively 51% and 49%. The correlations of the PCs are 0.78 and 0.68.

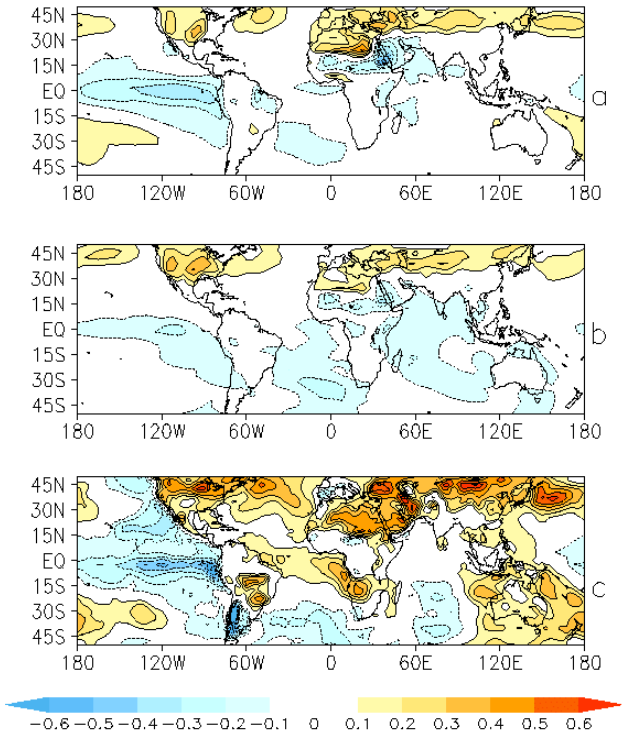

Figure 3. **a**) Regression of SAT onto the PC of the MSLP pattern of the SVD mode for the forced SST integrations. **b**) As a but with a 10-year running mean applied. c) As **a** but now for the NCEP/NCAR reanalysis and CMAP data. The covariances are normalized by the variances of the PCs. The contour interval is 0.1 K. For the SST forced runs all responses larger than 0.1 K are significant according to the 99% threshold of a t-test. Due to the shortness of the NCEP/NCAR and CMAP data the results are only significant according to the 80% threshold.

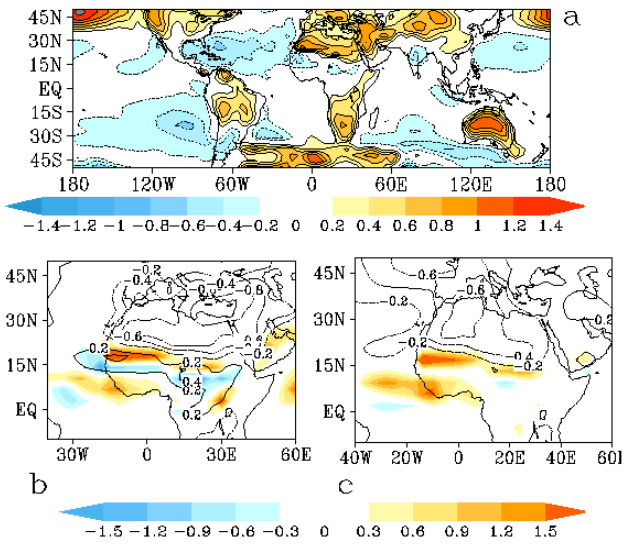

Figure 4. Coupled integrations: **a**) Difference in SAT [K] during JAS between 2050-2080 and 1950-1980. For SAT the global average mean between 50°S and 50°N is subtracted from it. **b**) Difference in rainfall [mm day^{-1}] (shaded) and MSLP [hPa] (contours) during JAS between 2050-2080 and 1950-1980. **c**) As **b** but now for the difference between the run with the Sahara heating and the control run (see text). The rainfall and MSLP have been reduced by a factor 2 to facilitate comparison with **b**.

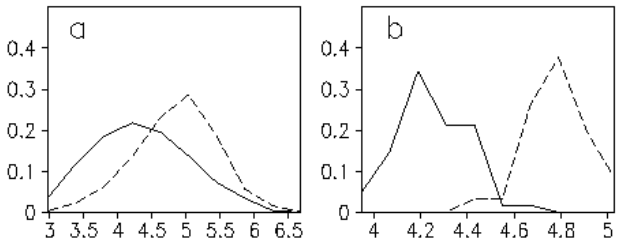

Figure 5. **a**) Probablity density function of JAS rainfall [mm day^{-1}] for the region 10^{o}N-20^{o}N, 10^{o}W-30^{o}E. Solid curve: 1950-1980. Dashed curve: 2050-2080 **b**) As **a** but 30-year averaged.